Evidence of Orographic Precipitation Suppression by Air Pollution–Induced Aerosols in the Western United States

DANIEL ROSENFELD AND AMIR GIVATI

The Hebrew University of Jerusalem, Jerusalem, Israel

(Manuscript received 6 September 2005, in final form 10 November 2005)

ABSTRACT

Analyses of trends of the orographic winter precipitation enhancement factor Ro along the coastal mountain ranges of the west coast of the United States show a pattern of decreasing Ro during the last century by as much as −24% from the southern border to central California, to no decrease in northern California and Oregon, and to a renewed decrease of Ro (−14%) in Washington to the Seattle area east of the Puget Sound. Similar decreases also occurred well inland, over Arizona, New Mexico, Utah (this study), and the east slopes of the Colorado Rockies (already documented prior to this study). Both absolute precipitation amounts and Ro are affected by fluctuations in the atmospheric circulation patterns, such as those associated with the Pacific decadal oscillation and the Southern Oscillation index. However, these climatic fluctuations cannot explain the observed trends in Ro. Although the trends of aerosols are available only since 1988, aerosol measurements from the Interagency Monitoring of Protected Visual Environments (IMPROVE) aerosol monitoring network show that negative trends in Ro are associated with elevated concentrations of fine aerosols [particulate matter less than 2.5 μm in diameter (PM 2.5)]. The PM 2.5 showed stability or some increase in the areas where their levels were elevated and decreasing trends of Ro were noted. Strong decreasing trends of the coarse aerosols (PM 10–PM 2.5) were noted, especially in the areas with elevated levels of PM 2.5. The decreasing trend in coarse aerosols (the coarse aerosols may act to initiate and enhance precipitation), in conjunction with the constancy and/or increases of the small aerosols (small aerosols suppress precipitation), can explain the continuing decreases in orographic precipitation during the last two decades despite the indicated improvement in the conventional air quality standards.

1. Introduction

It was recognized more than 40 years ago that continental clouds have larger "colloidal stability" than maritime clouds (Squires 1958). Laboratory experiments of relevance to coalescence in clouds in cloud condensation nuclei (CCN)-rich and -lean environments (Gunn and Phillips 1957) led to the suggestion that highly continental clouds, which form in a CCN-rich atmosphere, would produce less precipitation. Smoke from burning vegetation as well as urban and industrial air pollution serve as small CCN that form large concentrations of small cloud droplets. This in turn suppresses the drop coalescence and the warm-rain processes, as well as the ice precipitation (Rosenfeld 2000; Borys et al. 2003; Andreae et al. 2004), and thus prolongs the time required to convert the cloud water that exists in small drops into large hydrometeors that can precipitate. On the other hand, precipitation-forming processes can be accelerated with the addition of large (>1 μm) hygroscopic CCN. These CCN can occur naturally in the form of salt from sea spray (Rosenfeld et al. 2002), salty dust from desert playas (Rudich et al. 2002), air pollution emissions from paper mills (Eagen et al. 1974), or even artificial hygroscopic cloud-seeding materials (Silverman 2003).

Precipitation can be shut off completely because of high concentrations of small-aerosol polluting clouds with top temperatures >−10°C (Rosenfeld 1999, 2000; Rosenfeld and Woodley 2003). The suppression of the precipitation-forming processes does not necessarily always lead to a net reduction of precipitation. The delay of early precipitation in deep convective clouds with warm bases, such as those that occur in the Tropics and the southeast United States in the summer, can lead to

Corresponding author address: Daniel Rosenfeld, Institute of Earth Sciences, The Hebrew University of Jerusalem, Jerusalem 91904, Israel.
E-mail: daniel.rosenfeld@huji.ac.il

© 2006 American Meteorological Society

their invigoration and to overall additional precipitation (Andreae et al. 2004; Khain et al. 2005), mainly because of the dynamic response of the cloud development to the delayed precipitation.

In orographic clouds, the slowing of the conversion rate of cloud water into precipitation would be manifested as a net reduction of surface precipitation, because orographic clouds are often shallow and short lived because of their forced termination downwind of the topographic ridgeline. Borys et al. (2003) showed that the addition of as little as 1 μg m^{-3} of sulfate aerosols to a clean background can reduce the orographic snowfall rate in the Colorado Rocky Mountains by up to 50%, resulting from suppression of the riming of ice crystals with the smaller cloud droplets.

Suppression of orographic precipitation by anthropogenic aerosols is expected to be quite abundant, especially on the west coast of the continents in the subtropics and midlatitudes, where the precipitation over hills is a major source for the scarce water found there. Pristine air that comes from the ocean becomes polluted over the densely populated coastal plains before ascending over the downwind hills, where the pollution can have its detrimental effect on the precipitation. Givati and Rosenfeld (2004, 2005) related observed trends of decreasing orographic precipitation to the possible microphysical effects of pollution aerosols. They defined the suppression of orographic precipitation as a reduction in the orographic enhancement factor Ro, where Ro is defined as the ratio between the precipitation amounts over the hills to the precipitation amounts in the upwind lowland. Givati and Rosenfeld (2004) quantified for the first time the rainfall losses over hills and mountains downwind of major coastal urban areas in California and Israel. The suppression rate was found to be 15%–25% of the annual precipitation in hilly areas in California and Israel (Givati and Rosenfeld 2004, 2005). They showed that the suppression occurred mainly in the relatively shallow orographic clouds within the cold air mass of cyclones, and not in warm air masses. The Ro time series for relatively pristine areas crosswind to the polluted areas did not show any trend with time, and so served as controls to the polluted areas. Furthermore, Givati and Rosenfeld (2005) showed that the clouds that were most susceptible to the detrimental effects of air pollution over the hills in northern Israel were also the clouds for which glaciogenic cloud seeding caused the greatest rain enhancement. Givati and Rosenfeld (2005) suggest that it is reasonable to expect that clouds that are most sensitive to rain suppression because of aerosols that slow the rate of conversion of cloud droplets into precipitation particles would also be the clouds that would react most positively to cloud seeding that accelerates that rate.

Griffith et al. (2005) indicated similar reductions in mountainous precipitation in Utah and Nevada in a work that followed the approach utilized in the study of Givati and Rosenfeld (2004). They examined the ratio of winter precipitation between valleys to mountain precipitation downwind of the Salt Lake City and Provo, Utah, metropolitan complexes. The ratio of precipitation at mountain stations that are located in rural settings in Utah and Nevada remained stable (Griffith et al. 2005), supporting the role of pollution aerosols in decreasing Ro over the mountains to the east of Salt Lake City. While the decreasing trends of Ro in Utah occurred on the western slopes in precipitation that fell during westerly wind flows, similar decreasing trends in Ro of up to 30% were noted on the eastern slopes of the Rocky Mountains during easterly flows, downwind of Denver and Colorado Springs, Colorado (Jirak and Cotton 2006). It is difficult to explain how a change in the atmospheric circulation patterns could explain the decreasing trends of the orographic enhancement factor during both westerly and easterly winds over the respectively facing slopes, preferentially downwind of major urban areas. The temporal changes in aerosols remain the most plausible explanation.

With this background, the objectives of this study are as follows: 1) to examine the suppressive effect of aerosols on precipitation on a larger scale than California or Israel by looking at the ratio between the precipitation amounts over the hills to the precipitation over the upwind lowland areas in the western United States, from the Pacific coast inland to the Rocky Mountains; 2) to account for any variability that might be because of climatic fluctuations of the atmospheric circulation patterns; and 3) to relate the indicated trends in precipitation to trends in aerosol properties.

2. The study areas and method

a. Measuring the precipitation ratio of hilly-to-plains rain gauges

Following the methodology of Givati and Rosenfeld (2004, 2005) pairs of hilly and plains rain gauges (or clusters of gauges) were chosen for different areas across the western United States. To encompass the multidecadal scales of the longest periods of climatic fluctuations, we concentrated on the pairs with the longest available records. In addition to the long record, we required that the precipitation be highly correlated between the two gauges and that the precipitation at the higher-elevation rain gauge be considerably greater than the precipitation at the low-lying rain

gauge. In addition, the low-lying precipitation gauge should be upwind of the higher precipitation gauge in most circumstances. The high correlation is required for using the low stations to predict the "natural" rainfall in the hilly station. The large orographic enhancement factor indicates that much of the rainfall at the high station is generated by the orographic uplift of the air that comes from the region represented by the upwind lower-elevation station. For each pair of stations the trend of the ratio between the mountains and the plains was tested. This was done for both urban and rural pairs of rain stations. The nearby rural lowland–hill ratios to the side wind of the urban pairs and in the same airflow were used as control areas for the precipitation trend analysis of the urban pairs.

b. Population growth in western United States during the twentieth century

Many counties in the mountainous areas of the western United States are experiencing rapid growth in population (Booth 1999). The population of the southwestern United States has increased by approximately 1500% between 1900 and 1990, while the population of the United States as a whole has grown by just 225%. Arizona had the fastest growth in population of 2880%, followed by Nevada and Utah. Maricopa County (Phoenix), Arizona, had a 100-yr growth rate of 10 275%, with most of that growth occurring between 1960 and 1990 (Chourre and Wright 1997). The four fastest-growing states in the United States between 1990 and 2000 were Nevada (66.3% gain), Arizona (40%), Colorado (30.6%), and Utah (29.6%). The U.S. total population growth in the same period was only 13.2% (U.S. Census Bureau 2004a). This trend continued also between 2000 and 2004 (U.S. Census Bureau 2004b).

c. Precipitation characteristics in the western United States

The main precipitation source in the western United States during the winter is storms coming from the Pacific Ocean with mainly westerly winds (Davis and Walker 1992). Most of the precipitation falls on the windward slopes of mountain ranges. During summer the polar vortex contracts and the Pacific high expands and moves northward. This limits frontal precipitation along the west coast, but precipitation produced by local convection occurs in many areas well inland. The dominant circulation that creates summer precipitation is advection of air from the Gulf of Mexico, mostly during July and August, which is called the "summer monsoon" (Davis and Walker 1992). Because the character of the precipitation in the western United States is different between summer and winter, the analysis was done separately for wintertime (October–May) and summertime (June–September) series. We expected that the aerosols would affect the summer convective and the winter orographic precipitation differently. The thermally driven summer convective clouds are deeper and more long lived than the winter orographic clouds, and therefore are not as susceptible to the precipitation suppressive effects of small aerosols. Model simulations showed that enhanced concentrations of small CCN would still reduce the precipitation amounts from cold-based convective clouds, but the effect reverses for warm-based clouds, which actually produce more precipitation when polluted because of the delay of the early warm rainout (Khain et al. 2005).

In this study, we analyze pairs of upwind plain gauges versus downwind hilly rain gauges in conjunction with the measured aerosols at the locations presented in Fig. 1. Table 1 provides the details for these rain gauges, and Table 2 provides the locations of the Interagency Modeling of Protected Visual Environments (IMPROVE) aerosol monitoring stations used in this study.

3. Aerosol properties and trends

The underlying assumption of the previous studies (Givati and Rosenfeld 2004, 2005) was that the trend of Ro encompassed the period of main growth of the population, so that the overall emissions at the end of the period are larger than those at the beginning of the measured period, although not necessarily requiring a monotonic growth throughout the analysis period. Respectively, the overall precipitation suppression was evaluated as ending/starting values of Ro, as calculated using a simple linear regression line of Ro as a function of year. Air pollution indices showed recovery (decreasing trend) in California after the Clean Air Act was legislated in 1977, but Ro continued to decrease, and certainly did not show any recovery since then. Givati and Rosenfeld (2004) suggested that the there has been no decrease in the concentrations of small CCN, which are responsible for the suppression of precipitation, and pointed out the large increase in diesel consumption as a possible source of increasing production of such aerosols.

The current study expands the scope to the whole western United States to both pristine and polluted areas. Analyses of aerosol properties and trends are expanded in order to be correlated with the observed trends of precipitation, based on the IMPROVE monitoring program. Aerosol mass concentrations and composition during the winter months (October–March)

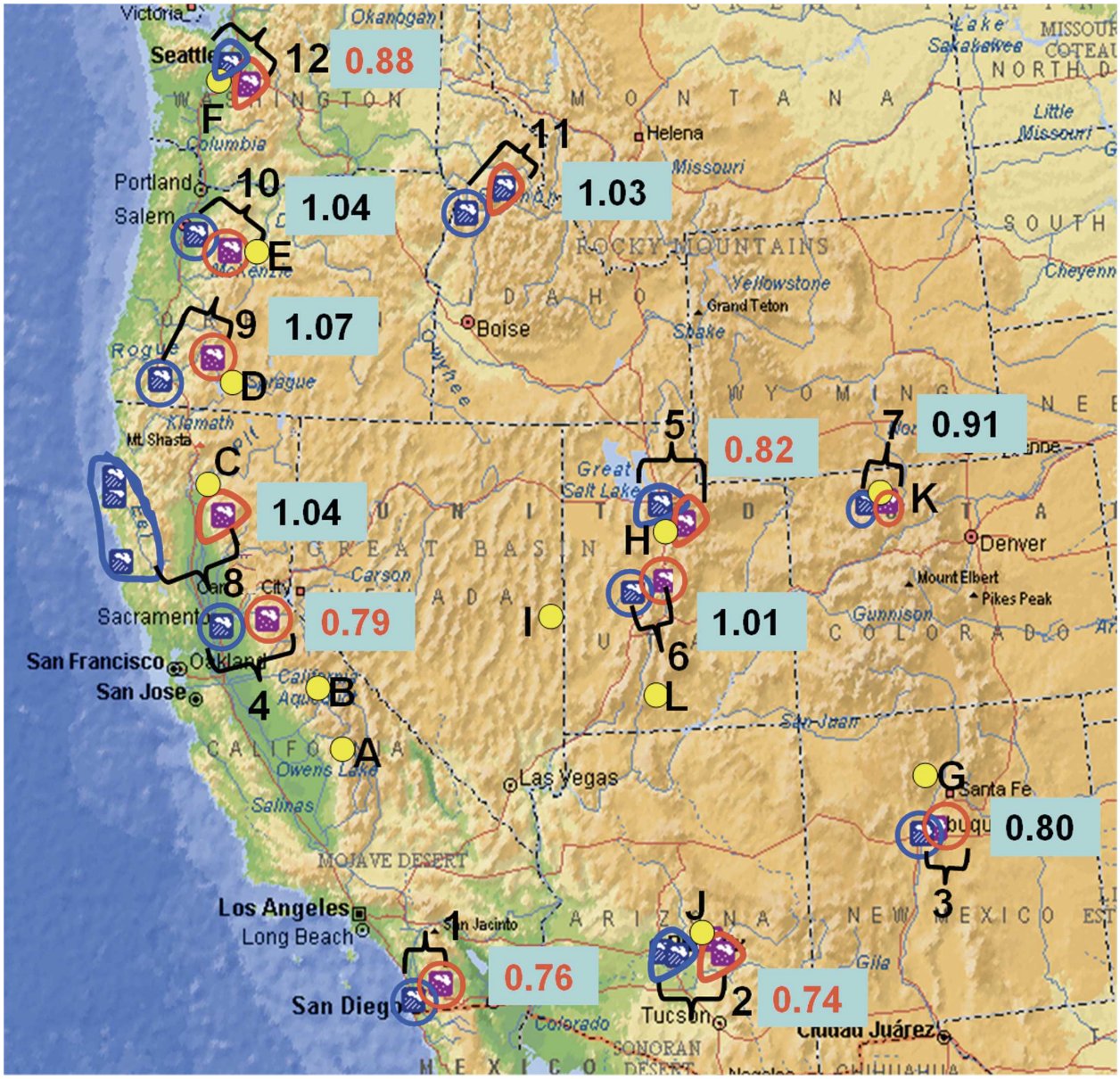

FIG. 1. Summary map of the locations of the rain gauges, aerosol monitoring stations, and the main results of the orographic precipitation. Rain gauge pairs are marked with a blue circle for the low station and a red circle for the downwind hilly station. Clusters of gauges are shown by an irregular enclosure. The station pairs are numbered and the respective details are provided in Table 1. The fractional change of the winter (October–May) orographic enhancement factor of the high rain gauge(s) with respect to the low rain gauge(s) that was indicated during the measurement period is shown near each pair. The red numbers are smaller than 1.00 with a statistical significance of $P < 0.05$; P is the statistical significance that corresponds to the Student's t test statistic, which measures the probability that there is no trend. The locations of the IMPROVE aerosol monitoring stations are shown in the yellow circles and are marked by characters respective to the reference in the text and the station details in Table 2.

were obtained for the areas of interest for the 1988–2003 (data are available online at http://vista.cira.colostate.edu/improve/). The trends were calculated using the tool provided at the IMPROVE Web site (online at http://vista.cira.colostate.edu/views/web/AnnualSummaryDev/Trends.aspx).

This tool provides quarterly averaged values of the parameters. The annual "winter" value is the average of the first and last quarters for that year. The trends of the mass concentration of the particles smaller than 2.5 μm [particulate matter (PM) 2.5] and of the particles with 2.5 $<$ diameter $<$ 10 μm (PM 10–PM 2.5)

TABLE 1. The locations and details of the plains and hilly rain gauge pairs and clusters, as numbered in Fig. 1. Clusters of gauges appear under the same pair number.

Pair No.	Data since	State	Plains stations	Lat (°)	Lon (°)	Elev (m)	Hilly stations	Lat (°)	Lon (°)	Elev (m)
1	1888	CA	San Diego	32.44	−117.10	10	Cuyamaca	32.59	−116.35	1557
2	1914	AZ	Litchfield Park	33.30	−11.222	343	Miami	33.24	−110.53	1200
2		AZ	Sacaton	33.05	−111.45	427	Roosevelt	33.40	−111.09	733
2		AZ	Mesa	33.25	−111.52	410				
2		AZ	Goulds Ranch	33.23	−112.04	400				
3	1945	NM	Albuquerque	35.03	−106.37	1770	Sandia Crest	35.13	−106.27	3563
4	1945	CA	Sacramento	38.31	−121.30	8	Pacific House	38.75	−12.050	1147
5	1949	UT	Tooele	40.32	−112.18	1607	Silver Lake	40.36	−111.35	2903
5		UT	Salt Lake City/Garfield	40.43	−112.12	1437	Alta	40.36	−111.38	2903
5		UT					Cottonwood	40.37	−111.47	1653
6	1945	UT	Delta	39.23	−112.31	1587	Levan	39.33	−111.52	1770
7	1948	CO	Hayden	40.29	−107.15	2127	Steamboat Springs	40.30	−106.50	2257
8	1949	CA	Eureka	40.48	−124.10	3	Mineral	40.35	−121.60	1627
8		CA	Scotia	40.29	−124.06	5	De Sabla	39.52	−121.37	907
8		CA	Fort Bragg	39.27	−123.48	3				
9	1949	OR	Grant pass	42.26	−123.19	310	Crater Lake	42.54	−122.08	2160
10	1954	OR	Stayton	44.48	−122.46	157	Marion Forks	44.37	−121.57	817
11	1958	ID	Riggins Ranger	45.25	−116.19	600	Elk City	45.49	−115.26	1327
11		ID					Headquarters	46.38	−115.48	1047
12	1949	WA	Seattle	47.36	−122.20	3	Palmer	47.18	−121.50	300
12		WA	Kent	47.23	−122.14	10				
12		WA	Puyallup	47.12	−122.20	17				

were calculated and are presented in Fig. 2. In addition, the trends of the following components of the fine particles were plotted: combined ammonium nitrates and sulfates, combined elemental and organic carbon, and soil materials. It is assumed here that small CCN concentrations are correlated positively with the mass of the soluble fraction of the fine particles, and hence act to suppress precipitation. Small CCN concentrations

TABLE 2. The locations of the IMPROVE aerosol monitoring stations used in this study.

Station	State	Code	Site name	Lat (°)	Lon (°)	Elev (m)
A	CA	SEQU1	Sequoia	36.489	−118.829	519
B	CA	YOSE1	Yosemite	37.712	−119.704	1603
C	CA	LAVO1	Lassen	40.540	−121.578	1732
D	OR	CRLA1	Crater Lake	42.896	−122.136	1966
E	OR	THSI1	Three Sisters	44.291	−122.043	885
F	WA	PUSO1	Puget Sound	47.570	−122.312	97
G	NM	BAND1	Bandelier	35.780	−106.266	1988
H	UT	LOPE1	Lone Peak	40.445	−111.708	1768
I	NV	GRBA1	Great Basin	39.005	−114.216	2065
J	AZ	TONT1	Tonto	33.649	−111.109	775
K	CO	MOZI1	Mount Zirkel	40.538	−106.677	3243
L	UT	BRCA1	Bryce Canyon	37.618	−112.174	2481

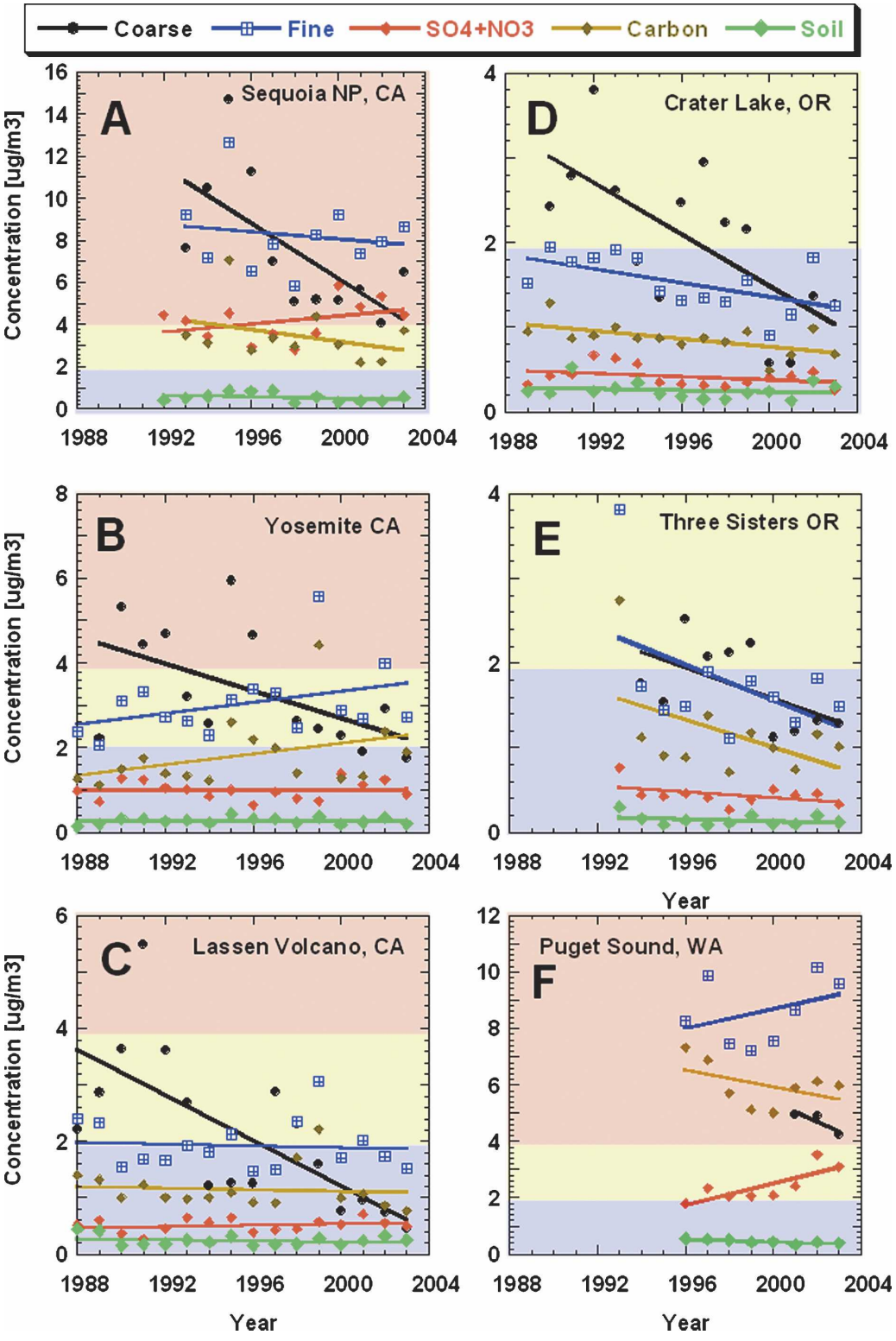

FIG. 2. Trends of coarse (2.5 μm < diameter < 10 μm) and fine (diameter < 2.5 μm) aerosols mass concentrations (μg m^{-3}) and their compositions as measured during winter (October–March) by the IMPROVE monitoring program. The composition of the fine aerosols is divided into mass of nitrates and sulfates (SO_4 + NO_3), organic and elemental carbon (Carbon), and crustal materials (Soil). The legend is provided at the top of the figure. The locations of the stations are marked with the respective letter on the map in Fig. 1 and are tabulated in Table 1.

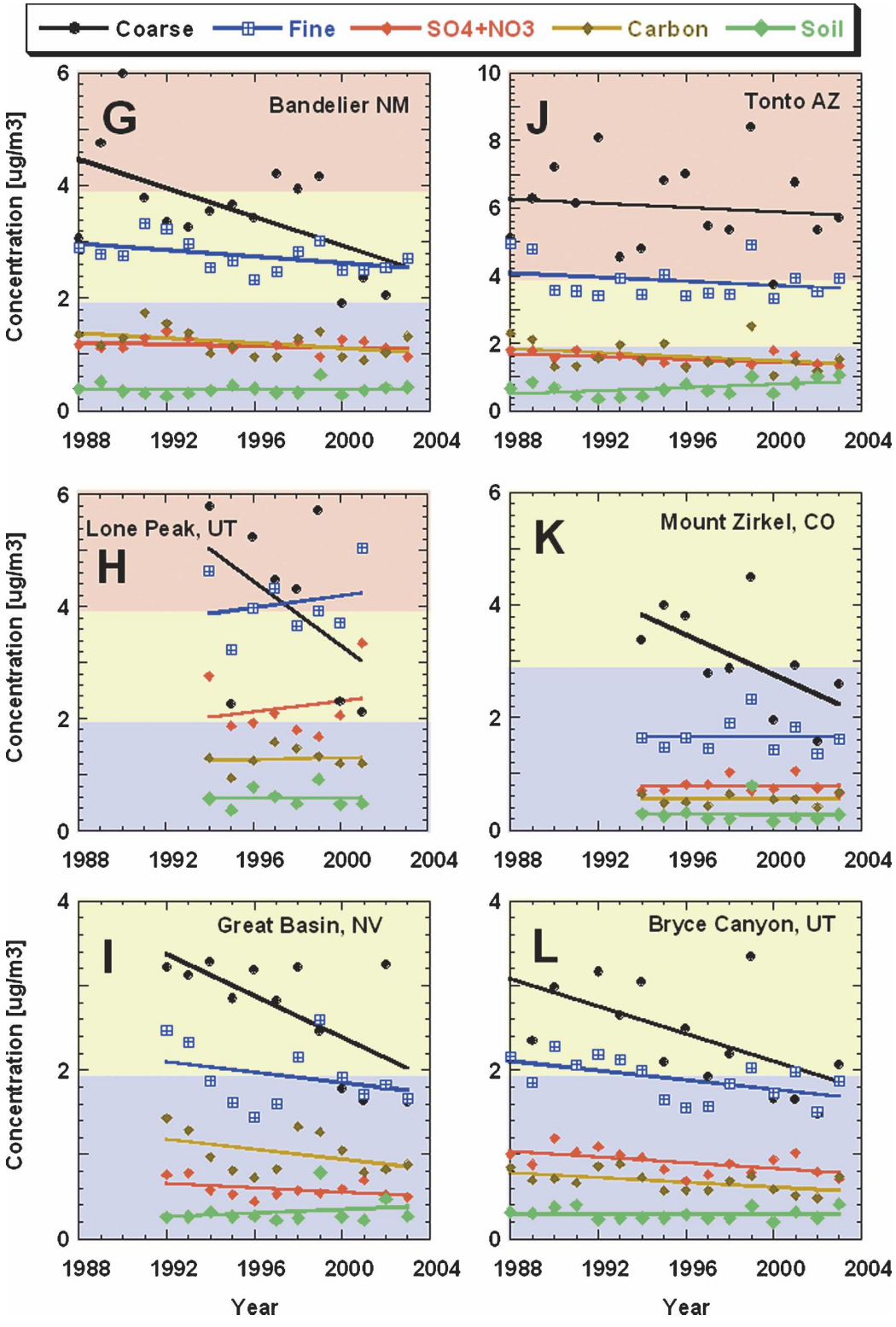

FIG. 2. (*Continued*)

are certainly positively correlated with the fine fraction of sulfates and nitrates; and are likely to be so with the carbonaceous aerosols after having time between emission and reaching the mountain ranges to chemically mature and develop some solubility. Soil particles constitute a small fraction of the fine particles, but probably a larger fraction of the coarse particles. No information is available in the IMPROVE data about the composition of the coarse fraction. However, even insoluble mineral particles can become hygroscopic by interacting with air pollution and becoming coated with soluble materials such as sulfates, and so act to enhance precipitation (Levin et al. 1996).

The analyzed IMPROVE stations were selected based on the availability of the longest possible time series of aerosol measurements that are geographically closest to representing the conditions at the higher-elevation gauge of the rain gauge pairs. The location of the selected IMPROVE stations are shown in Fig. 1, and their details are summarized in Table 2. The average aerosol concentrations probably differ considerably from those actually interacting with the clouds over the topographical barriers. However, we can assume that the levels and trends of the aerosol concentrations that interact with the clouds are correlated with those measured at the IMPROVE stations.

According to Fig. 2 the central Sierra Nevada region-(Sequoia and Yosemite, Figs. 2a and 2b) is much more polluted than the northern Sierra region (Lassen Volcano, Fig. 2c), in line with the strong decreasing trends of Ro in the central Sierra region, but not in the north, as reported by Givati and Rosenfeld (2004). Furthermore, while the coarse particles show a decreasing trend, the fine particles are stable at very high levels of 8.5 μm m^{-3} in the Sequoia area, mainly in the form of nitrates, sulfates, and organic carbon. The fine particle mass is smaller in Yosemite, probably because of the higher elevation of the monitoring station, but still shows a strong increasing trend mainly because of organic carbon (see the *P* values and the regression equations for the IMPROVE aerosol trends in Table 3). The decreasing trend of coarse aerosols that can have an enhancing effect on precipitation works in the same direction as the increasing trend of the fine aerosols that suppress precipitation. Coarse aerosol mass concentrations are decreasing also in the pristine areas in northern California and Oregon (Figs. 2c–e), but their concentrations are much smaller than in the central Sierra region (Figs. 2a and 2b). The concentration of the fine aerosols in these pristine areas is very small, and also is decreasing slightly. These fine aerosols are primarily composed of organic carbon, probably from residential wood stove combustion. Farther north in the

TABLE 3. The *P* values and the regression equations for the IMPROVE aerosol trends.

Site name	Sequoia	Yosemite	Lassen	Crater Lake	Three Sisters	Puget Sound
Station	A	B	C	D	E	F
Coarse *P* value	0.02	0.03	0.002	0.006	0.04	0.29
Coarse equation	$y = -0.6587x + 1322.7$	$y = -0.1599x + 322.4$	$y = -0.2007x + 402.65$	$y = -0.1522x + 305.82$	$y = -0.0919x + 185.4$	$y = -0.3475x + 700.38$
Fine *P* value	0.63	0.16	0.73	0.008	0.12	0.36
Fine equation	$Y = -0.0882x + 184.44$	$y = 0.0883x - 173.1$	$y = -0.0084x + 18.703$	$y = -0.0428x + 86.931$	$y = -0.1051x + 211.74$	$y = 0.1753x - 341.91$
$SO_4 + NO_3$ *P* value	0.13	0.83	0.98	0.46	0.13	0.01
$SO_4 + NO_3$ equation	$Y = 0.1423x - 280.12$	$y = 0.0061x - 11.071$	$y = 0.0062x - 11.926$	$y = -0.005x + 10.419$	$y = -0.0182x + 36.774$	$y = 0.1921x - 381.64$
Carbon *P* value	0.29	0.16	0.71	0.003	0.13	0.24
Carbon equation	$Y = -0.1413x + 285.84$	$y = 0.075x - 147.88$	$y = -0.0077x + 16.606$	$y = -0.0306x + 61.998$	$y = -0.0815x + 163.91$	$y = -0.15x + 305.93$
Soil *P* value	0.12	0.49	0.33	0.60	0.33	0.01
Soil equation	$Y = -0.0322x + 64.854$	$y = 0.0045x - 8.6615$	$y = -0.0049x + 10.064$	$y = -0.003x + 6.1666$	$y = -0.0063x + 12.682$	$y = -0.0246x + 49.73$

TABLE 3. (*Continued*)

Site name	Bandelier	Lone Peak	Great Basin	Tonto	Mount Zirkel	Bryce Canyon
Station	G	H	I	J	K	L
Coarse P value	0.01	0.27	0.02	0.66	0.07	0.04
Coarse equation	$y = -0.1273x + 257.48$	$y = -0.286x + 575.21$	$y = -0.1225x + 247.36$	$y = -0.0317x + 69.35$	$y = -0.1773x + 357.43$	$y = -0.0809x + 164$
Fine P value	0.07	0.59	0.34	0.30	0.94	0.02
Fine equation	$y = -0.0278x + 58.306$	$y = 0.0536x - 103.07$	$y = -0.0311x + 64.023$	$y = -0.0321x + 67.973$	$y = 0.0025x - 3.357$	$y = -0.028x + 57.816$
$SO_4 + NO_3$ P value	0.26	0.62	0.15	0.02	0.89	0.02
$SO_4 + NO_3$ equation	$y = -0.008x + 17.122$	$y = 0.0484x - 94.474$	$y = -0.0128x + 26.185$	$y = -0.0209x + 43.291$	$y = 0.0023x - 3.7425$	$y = -0.0171x + 35.025$
Carbon P value	0.08	0.80	0.17	0.18	0.81	0.02
Carbon equation	$y = -0.0224x + 46.014$	$y = 0.0081x - 14.888$	$y = -0.0288x + 58.567$	$y = -0.0309x + 63.333$	$y = 0.0032x - 5.9135$	$y = -0.0142x + 28.955$
Soil P value	0.67	0.87	0.46	0.05	0.88	0.84
Soil equation	$y = 0.0023x - 4.1211$	$y = 0.003x - 5.3562$	$y = 0.0105x - 20.629$	$y = 0.0239x - 47.041$	$y = -0.0032x + 6.7094$	$y = -0.0008x + 1.8509$

densely populated and industrial area of the Puget Sound (Fig. 2f) the air is polluted once more, with an increasing trend of the fine aerosols, mainly because of nitrates.

If these IMPROVE stations represent the conditions during orographic precipitation, it would be consistent with decreasing trends of orographic precipitation in central California, stable amounts from northern California to central Oregon, and then decreasing trends again in Washington to the east of the densely populated area of Seattle, around the Puget Sound.

Figure 2h shows that Lone Peak to the east of Salt Lake City has high concentrations of fine aerosols, with slightly increasing levels resulting from nitrate and sulfate, along with a decreasing trend of coarse aerosols. This is compatible with the reported strong decrease (−24% during 1949–2004) of orographic precipitation to the east of Salt Lake City (Griffith et al. 2005). The much cleaner air to the west and south (Great Basin and Bryce Canyon, Figs. 2i and 2l) is consistent with the reported stability of the orographic precipitation in these regions (Griffith et al. 2005).

4. Ro trend analysis for winter and summer precipitation

Figure 1 summarizes the results of the winter Ro trend analysis between hilly rain gauges versus relatively lower gauges upwind in different locations across the western United States. It can be seen that Ro has decreased significantly over the years (numbers in Fig. 1 are the end/start of the winter Ro as shown in Fig. 3) in all of the areas except for the pristine regions of northern California, Oregon, southern Idaho, and central Utah (regions 8, 9, 10, 11, and 6 in Fig. 1). The full statistics for all the pairs are provided in Table 4. Winter is defined here as being from October to May. The Ro values do not change much (most Ro values increase slightly) when restricting winter to October–March, so that the IMPROVE aerosols and rain gauges pertain exactly to the same months.

Figure 3 shows the winter and the summer Ro trends for gauges located in the Phoenix, Arizona, area (number 2 in Fig. 3), Albuquerque, New Mexico (3), Salt Lake City, Utah (5), Levan, Utah, (6) Steamboat Springs, Colorado (7), and Seattle, Washington (12). The trends for additional polluted areas in California can be found in Givati and Rosenfeld (2004). While the Ro for the winter orographic precipitation (shallow, short-lived clouds) is decreasing, the same pairs of gauges show almost a stable trend for the summer precipitation (deep convective, long-lived clouds). Those findings are in agreement with what we found for many

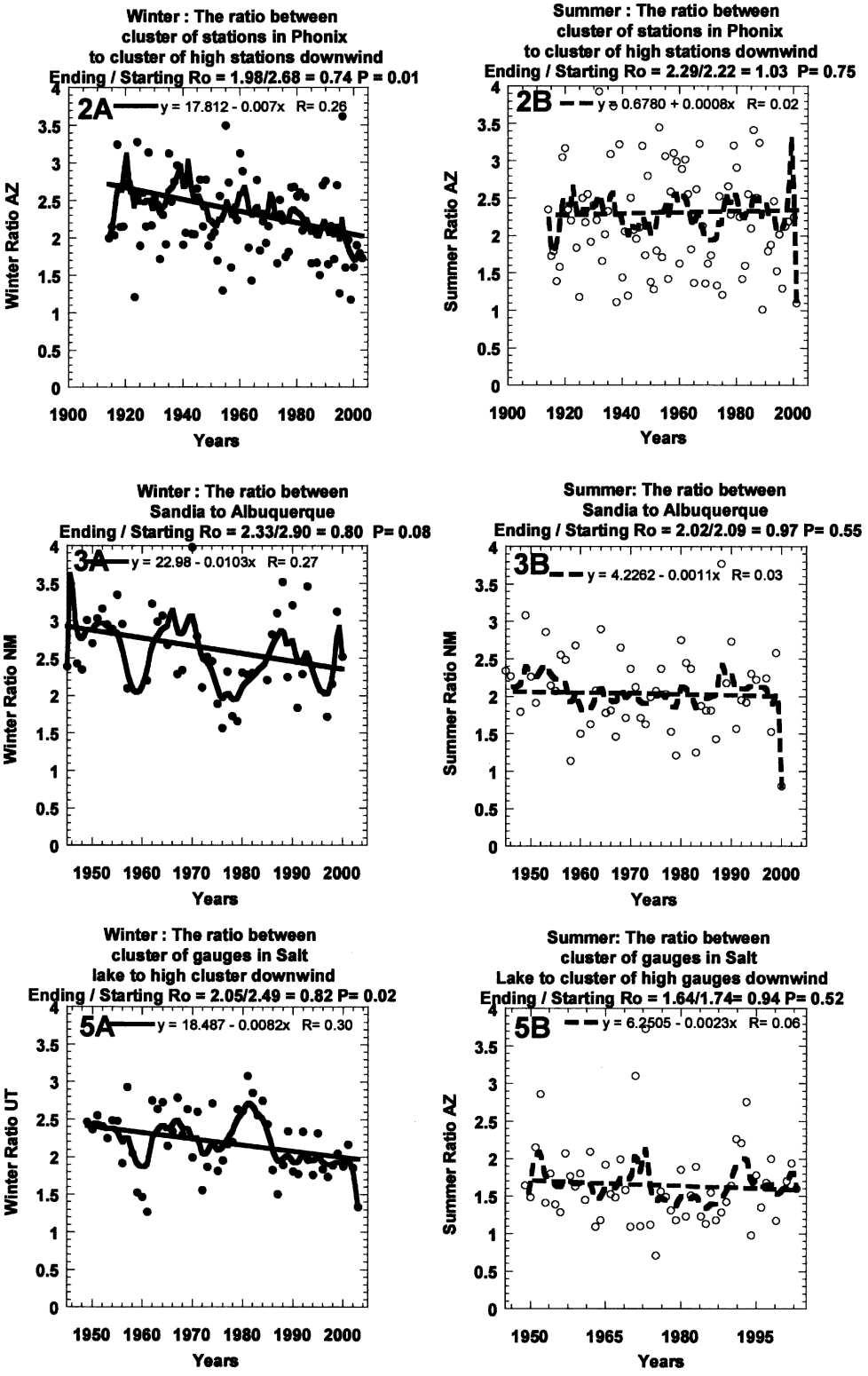

FIG. 3. Trend analysis for (left) winter and (right) summer ratio of precipitation measured in a cluster of gauges in the Phoenix area vs the downwind hilly cluster of gauges (2A and 2B), Albuquerque vs the Sandia crest (3A, 3B), a cluster of gauges in Salt Lake City vs those in the downwind hilly cluster of gauges (5A, 5B), Levan vs Delta (6A, 6B), Steamboat vs Hayden (7A, 7B) and a cluster of gauges in the Seattle area vs the downwind hilly gauge in Palmer (12A, 12B). Note the sharp decrease in Ro of winter precipitation with time in areas that are affected by urban air pollution, whereas the Ro of summer precipitation remains stable.

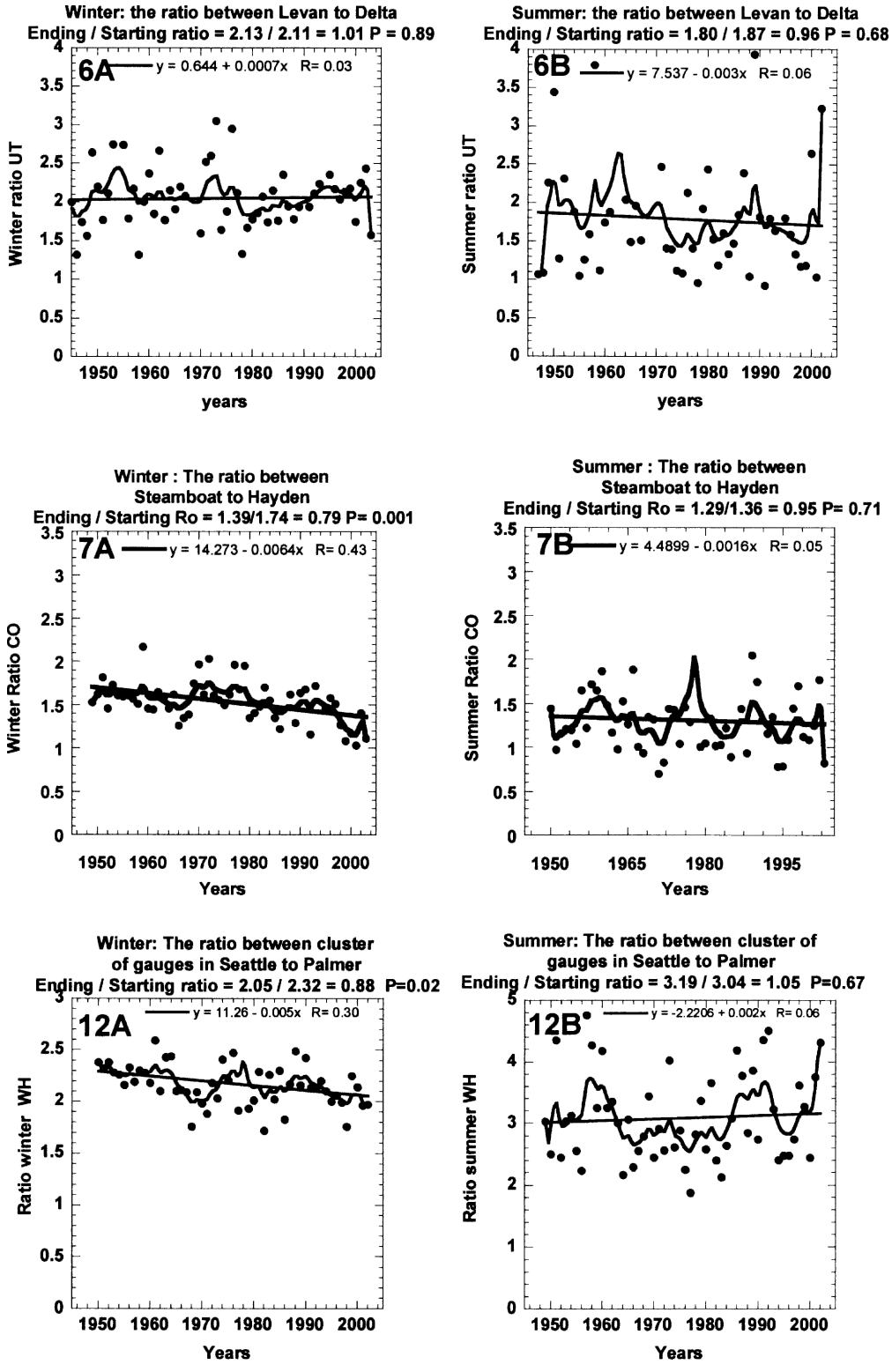

FIG. 3. (*Continued*)

TABLE 4. Rain gauge details and summary of the Ro trend analysis for winter and summer precipitation. The asterisk is explained in the text. The double asterisk indicates that values are annual rather than for winter or summer. "Station name" is the rain gauge name or the cluster name, and the pair number as appearing on Fig. 1; "Years" is the period of precipitation measurements; "Avg winter/summer precipitation" is the average amount of precipitation (mm yr^{-1}) at each station for the winter (October–May) and summer (June–September) periods; "Correlation" is the correlation for the winter or the summer precipitation between the plains and the hilly gauge readings; "Ending/starting ratio" is the ratio (where the ratio is defined as the ratio between the precipitation amounts at the hills and at the upwind lowland) in the beginning of the time series in comparison with the ratio at the end of the time series (the change) as calculated using the regression line (the trend along the years); "*P* value" is the statistical significance of the trend and corresponds to the Student's *t* test statistic, which quantifies the chance that there is no trend; "Equation" is the regression equation used to calculate the trend.

Station name	1: San Diego	1: Cuyamaca	2: Phoenix cluster	2: Cluster downwind of Phoenix	3: Albuquerque	3: Sandia
State	CA	CA	AZ	AZ	NM	NM
Lat, lon (°)	32.44, −117.10	32.59, −116.36	33.20, −111.80	33.30, −111.22	35.03, −106.37	35.13, −106.27
Years	1888–2003		1914–2003		1945–2000	
Elev (m MSL)	3	1550	395	970	1170	3563
Avg winter precipitation (mm)	290*	875*	130	283	107	254
Avg summer precipitation (mm)			80	164	123	246
Correlation winter	0.80		0.89		0.82	
Correlation summer			0.69		0.61	
Ending/starting ratio winter	3.28/4.32 = 0.76		1.98/2.68 = 0.74		2.33/2.90 = 0.80	
Ending/starting ratio summer			2.29/2.22 = 1.03		2.02/2.09 = 0.97	
P value winter	0.003		0.01		0.08	
P value summer			0.75		0.55	
Equation winter	$y = 20.871 - 0.008x$		$y = -0.0079x + 17.81$		$y = -0.0103x + 22.938$	
Equation summer			$y = 0.6780 + 0.000\,82x$		$y = 4.223 + 0.001x$	

Station name	4: Sacramento	4: Pacific House	5: Salt Lake cluster low	5: Cluster downwind to Salt Lake	7: Hayden	7: Steamboat Springs
State	CA	CA	UT	UT	CO	CO
Lat, lon (°)	38.35, −121.30	38.750, −120.50	40.37, −112.15	40.36, −111.40	40.29, −107.15	40.30, −106.50
Years	1945–2002		1949–2003		1948–2002/1997	
Elev (m MSL)	8	1147	1521	2487	2126	2257
Avg winter precipitation (mm)	475*	1321*	342	748	292	445
Avg summer precipitation (mm)			152	227	170	209
Correlation winter	0.86		0.79		0.80	
Correlation summer			0.84		0.85	
Ending/starting ratio winter	2.48/3.15 = 0.79		2.05/2.49 = 0.82		1948–97: 1.50/1.65 = 0.91; 1948–2002: 1.36/1.71 = 0.80	
Ending/starting ratio summer			1.64/1.74 = 0.96		1.29/1.36 = 0.95	
P value winter	0.003		0.02		0.001/0.10	
P value summer			0.52		0.71	
Equation winter	$y = 35.863 - 0.017x$		$y = 18.487 - 0.0082x$		$y = 14.273 - 0.0064x$	
Equation summer			$y = 6.2504 - 0.0023x$		$y = 4.899 + 0.0016x$	

TABLE 4. (*Continued*)

Station name	6: Levan	6: Delta	12: Seattle cluster low	12: Palmer	8: Northern California cluster	8: Northern California cluster downwind
State	UT	UT	WA	WA	CA	CA
Lat, lon (°)	39.23, −112.31	39.33, −111.52	47.36, −122.20	47.18, −121.50	40.01, −123.88	38.583, −121.48
Years	1945–2003		1949–2003		1949–2000	
Elev (m MSL)	1585	1770	10	300	3	1270
Avg winter precipitation (mm)	280	144	812	1734	1090*	1550*
Avg summer precipitation (mm)	90	54	127	381		
Correlation winter	0.85		0.89		0.90	
Correlation summer	0.79		0.83			
Ending/starting ratio winter	2.13/2.11 = 1.01		2.05/2.32 = 0.88		1.43/1.37 = 1.04	
Ending/starting ratio summer	1.80/1.87 = 0.96		3.19/3.04 = 1.04			
P value winter	0.89		0.02		0.57	
P value summer	0.68		0.67			
Equation winter	$y = 0.644 + 0.0007x$		$y = 11.26 - 0.005x$		$y = 0.0011x - 0.6877$	
Equation summer	$y = -0.0026x + 7.537$		$y = -2.226x$			

Station name	9: Grants Pass	9: Crater Lake	10: Stayton	10: Marion	11: Riggins	11: Cluster high
State	OR	OR	OR	OR	ID	ID
Lat, lon (°)	42.26, −123.19	42.54, −122.08	44.48, −122.46	44.37, −121.57	45.25, −116.19	45.93, −115.37
Years	1949–2003		1954–2002		1958–2003	
Elev (m MSL)	310	2160	600	1187		
Avg winter precipitation (mm)	767**	1682**	422**	860**		
Avg summer precipitation (mm)						
Correlation winter	0.86**		0.91**		0.70**	
Correlation summer						
Ending/starting ratio winter	2.25/2.10 = 1.07**		1.39/1.34 = 1.04**		2.17/2.11 = 1.03**	
Ending/starting ratio summer						
P value winter	0.29**		0.20**		0.77**	
P value summer						
Equation winter	$y = -3.7154 + 0.0029x$**		$y = -1.3998 + 0.001\,34x$**		$y = -0.2165 + 0.001x$**	
Equation summer						

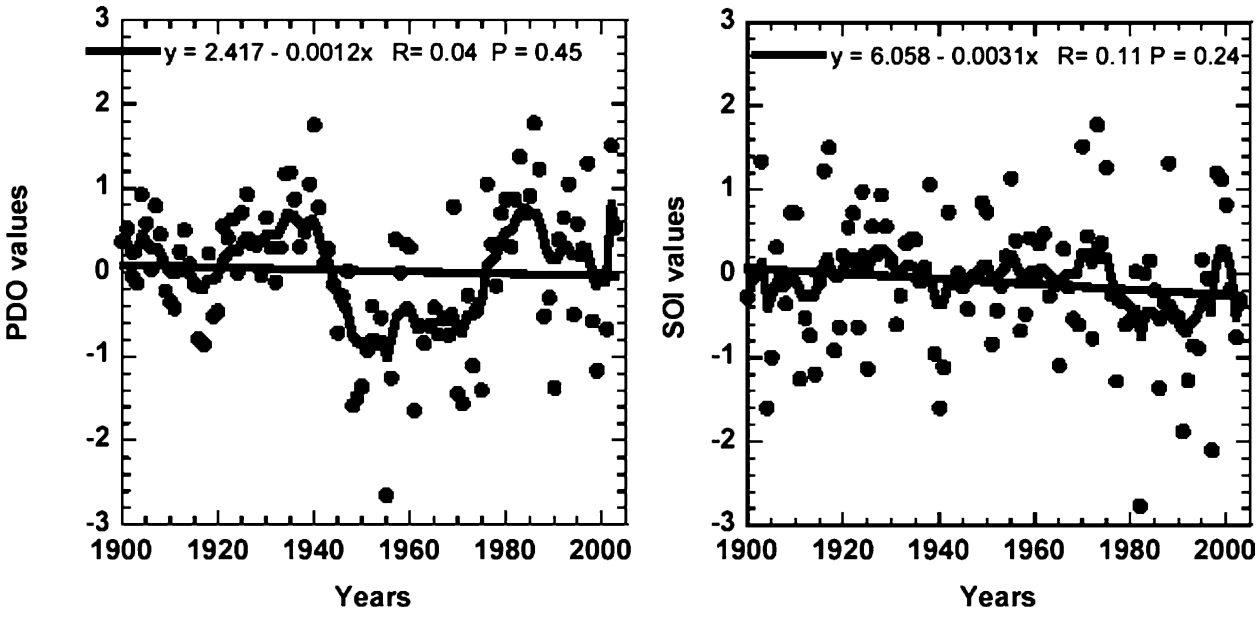

FIG. 4. Winter values (October–April) of the (left) PDO and (right) SOI indexes. Note the three phases of the PDO: positive from 1900 to 1944, negative from 1945 to 1975, and positive since 1976.

clustered hilly versus plains rain gauges in California and Israel (Givati and Rosenfeld 2004, 2005). Here we can also see that suppression of winter orographic precipitation occurs not only when maritime air is polluted over coastal urban areas, but also hundreds of kilometers farther inland. Table 4 provides the gauge details, correlations between the pairs/clusters of gauges, and summarizes the Ro trend analysis for all gauges from Fig. 1. No seasonal separation was done in areas with little summer precipitation, such as California (marked with an asterisk in Table 4).

5. Testing trends in climate indices as an alternative explanation for decreasing Ro

The most likely alternative explanation for the reduction in Ro is a decreasing trend in the cross-mountain component of the low-tropospheric wind velocity and moisture flux during rain events. Givati and Rosenfeld (2004) applied a radiosonde regression model and found that the relevant meteorological conditions during rainy days did not change systematically over the years, and that the observed trends in Ro are likely caused by nonmeteorological reasons, such as anthropogenic air pollution. Precipitation in the western United States may also be subject to climatic fluctuations like the El Niño–Southern Oscillation index (SOI) (Allan et al. 1991) and its multidecadal counterpart, the Pacific decadal oscillation (PDO) (Zhang et al. 1997; Mantua et al. 1997). The PDO index is defined as the leading principal component of the North Pacific monthly sea surface temperature variability. The PDO is a long-lived El Niño–like pattern of Pacific climate variability. The SOI is defined as the normalized pressure difference between Tahiti and Darwin (Ropelewski and Jones 1987). Figure 4 displays the winter values (October–April) of the PDO (Fig. 4a) (after Mantua et al. 1997) and the SOI (Fig. 4b) from 1900 to 2003. It can be seen that during this period the PDO had three phases: a positive (warm) phase from 1900 to 1944, a negative (cold) phase from 1945 to 1975, and another positive phase since 1976.

Dettinger et al. (2004) characterized the effects of the PDO and the SOI on the ratio of precipitation between mountains and plain areas in the California Sierra Nevada region. During negative PDO and positive SOI, the westerly wind component is stronger so that the mountain–plains orographic factor is higher than in the positive PDO phase (El Niño like). There is less overall precipitation in the negative than in the positive PDO phase (Dettinger et al. 2004). Figure 5 displays the relations between the PDO and SOI to the ratio between Cuyamaca and San Diego, California (Figs. 5a and 5b), and between Miami, and Phoenix (Figs. 5c and 5d). It can be seen that the Ro is weakly negatively correlated with the PDO, and even more weakly so with the SOI. These weak relations could still explain the indicated trends if the PDO and SOI would have large trends with time. This is not the case, however, as shown in the next section.

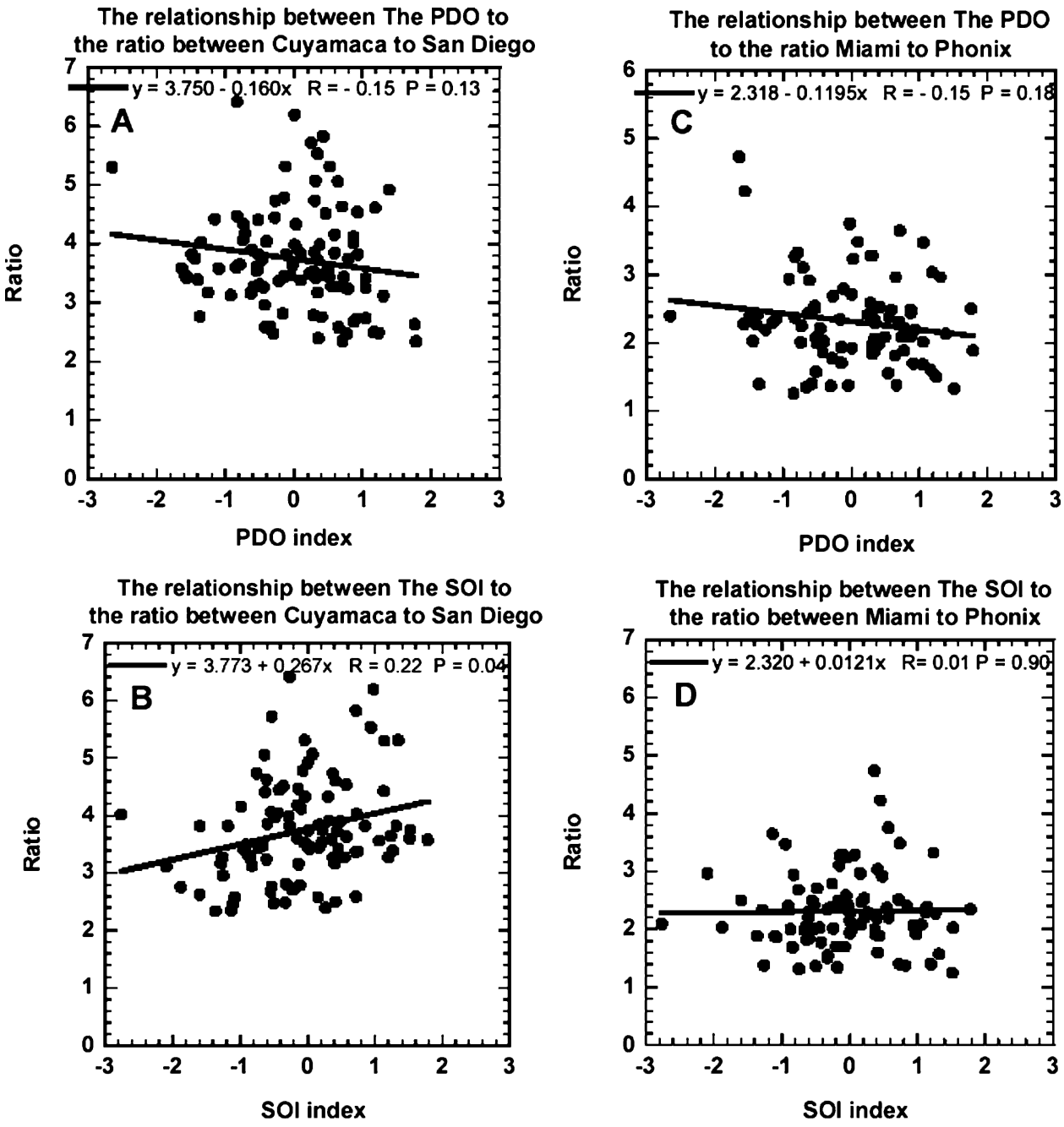

FIG. 5. The relationship of the (top) PDO and (bottom) SOI to the orographic enhancement factor (Ro) between (left) Cuyamaca and San Diego and between (right) Miami and Phoenix. Note the low correlation between the PDO and SOI and Ro.

To better understand the possible effects of those climate indices on the orographic precipitation in the western United States, we analyzed the hill–plain Ro of precipitation with respect to the winter values of the PDO and SOI. Pairs of hill–plain gauges with the longest record were chosen to test the climate indices fluctuations through the whole century.

Figure 6 presents the Ro of annual precipitation between hilly and plain stations for three pairs of stations with the longest available records: Cuyamaca–San Diego, Miami–Phoenix, and Lake Spaulding–Eureka, California. Figures 6a and 6b are for locations downwind of urban areas, while Fig. 6c represents a relatively pristine area. The Ro time series were tested with respect to three PDO categories: (Fig. 6a) PDO $<$ -0.5, (Fig. 6b) a neutral category of $-0.5 <$ PDO < 0.5,

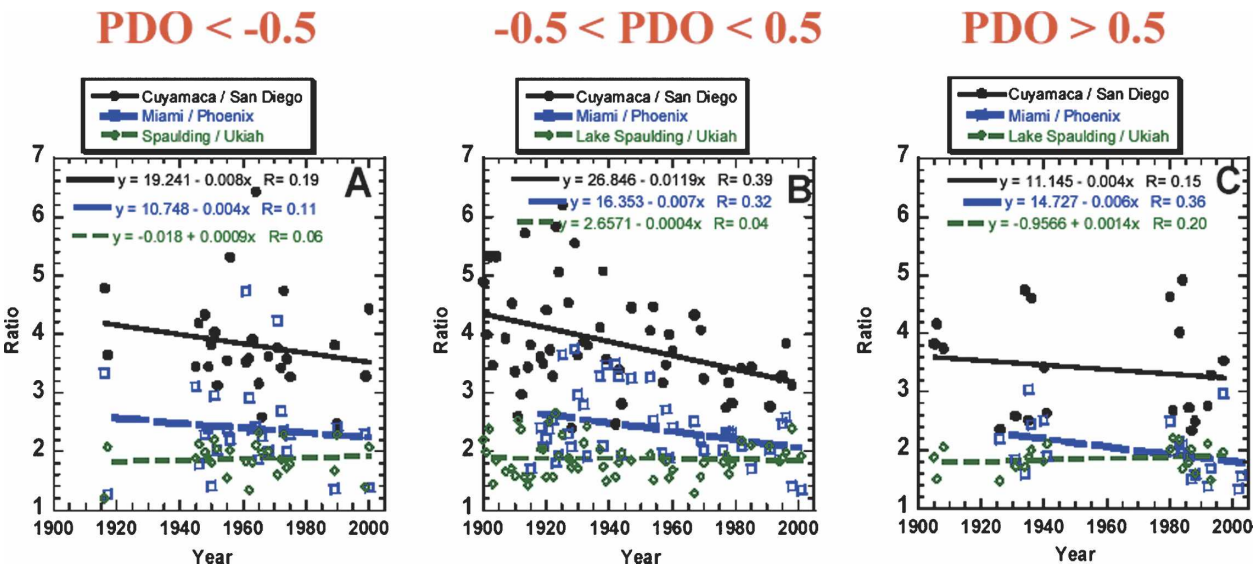

FIG. 6. The ratio of hilly–plain pairs of rain gauges in polluted areas (Cuyamaca–San Diego, Miami–Phoenix) and a relatively pristine area (Lake Spalding–Ukiah) for PDOs classified into the three indicated categories. The ratio for the polluted pairs decreases in all three PDO categories, whereas no trend is indicated for the ratio at the relatively pristine area.

and (Fig. 6c) PDO $>$ 0.5. It can be seen in the figure that the Ro between Cuyamaca and San Diego and between Miami and Phoenix decrease for all PDO categories, while the Ro in the pristine area (Lake Spaulding versus Ukiah) remains stable with time in all the PDO categories. In the polluted areas, suppression of orographic precipitation increases with time, regardless of the PDO category.

Figure 7 shows the same methodology but for the Ro of the station pairs with the longest records with respect to three SOI categories, as was done for the PDO. It can be seen that as with the PDO (Fig. 6), the Ro decreases for all SOI categories for the polluted pairs, but not for the relatively pristine one.

Tables 5 and 6 display the results of multiple linear regressions, where the precipitation amounts and the Ro are explained by variability in the PDO, SOI, and year as the three independent regression parameters. The dependent variables in the regressions were the individual precipitation amounts from the hilly and

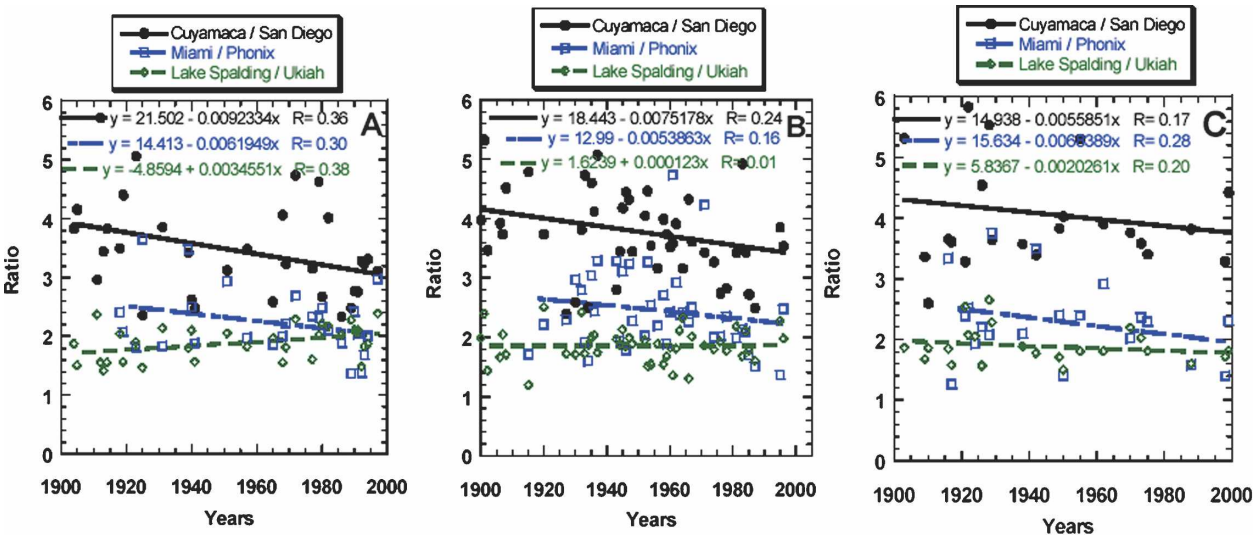

FIG. 7. Same as Fig. 6, but for SOI, classified into the same three categories from (a) to (c) as in Fig. 6. As in Fig. 6, the ratio for the polluted pairs decreases in all three SOI categories, whereas no trend is indicated for the ratio in the relatively pristine area.

TABLE 5. Multiple linear regression results showing the significances (P) of three independent variables (PDO, SOI, and year) vs the dependent variable (individual precipitation of rain gauges across the United States).

Station Name	State	PDO P value	SOI P value	Years P value
San Diego	CA	0.004	0.430	0.522
Cuyamaca	CA	0.005	0.175	0.287
Sacramento	CA	0.642	0.247	0.580
Pacific House	CA	0.358	0.972	0.835
Phoenix cluster	AZ	0.254	0.001	0.423
Cluster downwind to Phoenix	AZ	0.253	0.001	0.064
Albuquerque	NM	0.558	0.112	0.006
Sandia	NM	0.970	0.007	0.005
Salt Lake City cluster	UT	0.541	0.461	0.037
Cluster downwind to Salt Lake City	UT	0.528	0.539	0.519
Hayden	CO	0.479	0.576	0.580
Steamboat Springs	CO	0.851	0.820	0.588
Seattle cluster	WA	0.004	0.564	0.221
Palmer	WA	0.072	0.923	0.080

plains area rain gauges (see Table 5) and the Ro of precipitation amounts between those hilly and plains gauges (see Table 6). It can be seen in Table 5 that the PDO and the SOI do affect the precipitation amounts. For example, P values for the PDO effect on precipitation in San Diego and Cuyamaca are 0.004 and 0.005, respectively. Nonetheless, when we test the effect of the PDO and SOI not on the absolute precipitation amounts but on the ratio between them, no significant effect is found. The only variable that has a significant effect on the ratio is the year. The Ro decreases significantly over the years, even when the variability in the PDO and SOI is taken into account by the multiple regression model. The "years" variable represents another change that occurs with time and affects Ro. With the lack of any other alternative explanation of which we are aware, we suggest that the decreasing Ro with the years is likely the result of the increasing small CCN aerosols and possibly the decreasing of giant CCN in the form of coarse aerosols over the years.

TABLE 6. Multiple linear regression results showing the significances (P) of three independent variables (PDO, SOI, and year) vs the dependent variable (ratio of precipitation between the rain gauge pairs, which is the orographic enhancement factor Ro).

Pairs of stations	State	PDO P value	SOI P value	Years P value
Cuyamaca/San Diego	CA	0.430	0.100	0.005
Pacific House/Sacramento	CA	0.431	0.703	0.012
Phoenix cluster/cluster downwind	AZ	0.478	0.703	0.010
Albuquerque/Sandia	NM	0.577	0.451	0.153
Salt Lake City cluster/cluster downwind	UT	0.911	0.840	0.050
Steamboat Springs/Hayden	CO	0.110	0.216	0.083
Seattle cluster/Palmer	WA	0.394	0.419	0.0001

6. Discussion and conclusions

In this study, we expanded the analysis of the possible effects of air pollution on orographic precipitation from California to the whole western United States. Analyses of trends of the orographic enhancement factor Ro along the coastal mountain ranges of the whole west coast of the United States showed a pattern of decreasing Ro by as much as −24% from the south border to central California, no decrease from northern California to Oregon, and a renewed decrease (−14%) from Washington to the east of the Puget Sound. Both absolute precipitation amounts and Ro are affected by fluctuations in the atmospheric circulation patterns, such as those associated with the PDO and SOI. However, these climatic fluctuations could not explain the observed trends in Ro. A case in point is the decreasing trend of Ro in both the western (this study) and eastern (Jirak and Cotton 2006) slopes of the Rockies. It is difficult to imagine a trend in the circulation patterns that would result in such a trend.

Aerosol measurements since 1988 from the IMPROVE aerosol monitoring network in the west coast mountain ranges show that the negative trends in Ro were associated with elevated concentrations of fine aerosols (PM 2.5). The PM 2.5 showed stability or some increase in the areas where fine aerosols levels were elevated and decreased trends of Ro were noted. That increase came mainly from increasing nitrates and organic carbon that overcompensated for the decreasing trends in sulfates. In any case, there is certainly no indication of a decrease in the fine aerosols at the more polluted areas during the last two decades, which at least correspond to the lack of recovery of orographic precipitation in response to the recent efforts to reduce the air pollution.

Strong decreasing trends of the coarse aerosols (PM 10–PM 2.5) was noted, especially in the areas with elevated levels of PM 2.5. Coarse aerosols may enhance precipitation if they act as giant CCN. This is likely the case when the coarse particles interact with polluted air and are coated with soluble materials such as sulfates (Levin et al. 1996). If so, a decreasing trend in the concentrations of the coarse aerosols, in conjunction with stable or increasing concentrations of the small aerosols, might explain the continued trend of orographic precipitation losses during the last two decades, despite

the indicated decreases in PM 10, based on conventional air quality standards. It remains to be determined why coarse aerosols have been decreasing during the last two decades while fine aerosols remained stable or increased at the same time.

It has been assumed that air masses well inland would not be as pristine as those impacting the coastline during onshore flow, and therefore that the impacts of pollution aerosols on orographic precipitation well inland would be smaller. However, analyses of Ro over the inland mountains of the western United States all of the way to the Rockies shows that large decreases of Ro occur there (from −15% to −25%) in areas that are potentially affected by anthropogenic sources. The IMPROVE aerosol measurements show elevated levels of PM 2.5 in the areas that experienced decreasing trends of Ro, such as those to the east of Salt Lake City, Utah, Phoenix, and Albuquerque, New Mexico. Low aerosol levels were recorded in southwest Utah and Idaho where the Ro trends were stable. The extent of decrease in Ro at the northern Rockies is not certain because of the fact that the winters of 1998–2003 are responsible for most of the decrease (see panel 7A in Fig. 3). The decrease in Ro is contributed by the much-reduced values at Steamboat Springs, Colorado, with no obvious deviation at Hayden, Colorado, at the same time. No similar strong decrease in the recent years was indicated anywhere else in the gauges analyzed for this study. If the Ro that occurred in the northern Colorado Rockies really decreased, it was associated with rather low aerosol levels measured on Mount Zirkel. These low concentrations may mainly reflect the high altitude (3243 m) of the measuring station. Such low concentrations of PM 2.5 (averaging about 2 μm m^{-3}) do not exclude the possibility of long-range air pollution transport being responsible for the possible decrease in Ro. Measurements conducted on top of a nearby mountain of the same elevation (Borys et al. 2003) have shown that fine aerosol concentrations as low as 1 μm m^{-3} can cut the snow precipitation rate in half relative to pristine conditions. In any case, we should not expect a perfect match between the IMPROVE and rain gauge trends, because the IMPROVE aerosol data cover only the last two decades, whereas the trends in Mount Zirkel are mainly based on data from the previous decades.

Evidently, decreases in Ro occurred during winter orographic precipitation, but not during convective summer precipitation over the same mountain ranges. This is in line with the expectation that aerosol-induced changes in the rate of the conversion of cloud water to precipitation would result in a respective net change of surface precipitation in shallow and short-lived orographic clouds, but not necessarily in deeper and longer-living thermally driven convective clouds.

These reported findings suggest that anthropogenic air pollution has had a major impact on orographic precipitation well beyond the local scale of the pollution sources. It appears that air pollution suppresses much of the orographic precipitation over the western United States, which is responsible for most of the water resources in this semiarid part of the world. This is an issue with major economical and societal implications, not only to the United States, but also to many other densely populated parts of the world where the livelihood of the inhabitants depend on water from orographic precipitation, which might be compromised by the air pollution produced by the inhabitants. Examples of such densely populated semiarid areas that depend on orographic precipitation that is susceptible to air pollution produced by the local inhabitants include the Mediterranean basin, the west coast of the United States, the Middle East, Southeast Asia and China, and the southeastern part of Australia and South Africa.

Acknowledgments. The work described here was made possible in part by funding by the Public Interest Energy Research (PIER) Program of the California Energy Commission. The authors thank Dr. W. L. Woodley for valuable discussions and for reviewing the manuscript.

REFERENCES

Allan, R. J., N. Nicholls, P. D. Jones, and I. J. Butterworth, 1991: A further extension of the Tahiti–Darwin SOI, early ENSO results and Darwin pressure. *J. Climate,* **4,** 743–749.

Andreae, M. O., D. P. Rosenfeld, A. A. Costa, G. P. Frank, K. M. Longo, and M. A. F. Silva-Dias, 2004: Smoking rain clouds over the Amazon. *Science,* **303,** 1337–1342.

Booth, D. E., 1999: Spatial patterns in the economic development of the Mountain West. *Growth Change,* **30,** 384–405.

Borys, R. D., D. H. Lowenthal, S. A. Cohn, and W. O. J. Brown, 2003: Mountaintop and radar measurements of anthropogenic aerosol effects on snow growth and snowfall rate. *Geophys. Res. Lett.,* **30,** 1538, doi:10.1029/2002GL016855.

Chourre, M., and S. Wright, 1997: Population growth of the Southwest United States, 1900-1990. *Workshop on Impact of Climate Change and Land Use in the Southwestern Untied States, Human Impacts on the Landscape,* Tempe, AZ, U.S. Department of the Interior and U.S. Geological Survey, 1–8.

Davis, R. E., and D. R. Walker, 1992: An upper-air synoptic climatology of the western United States. *J. Climate,* **5,** 1449–1467.

Dettinger, M., K. Redmond, and D. Cayan, 2004: Winter orographic precipitation ratios in the Sierra Nevada—Large-scale atmospheric circulations and hydrologic consequences. *J. Hydrometeor.,* **5,** 1102–1116.

Eagen, R. C., P. V. Hobbs, and L. F. Radke, 1974: Particle emis-

sions from a large Kraft paper mill and their effects on the microstructure of warm clouds. *J. Appl. Meteor.,* **13,** 535–552.

Givati, A., and D. Rosenfeld, 2004: Quantifying precipitation suppression due to air pollution. *J. Appl. Meteor.,* **43,** 1038–1056.

——, and ——, 2005: Separation between cloud-seeding and air-pollution effects. *J. Appl. Meteor.,* **44,** 1298–1314.

Griffith, D. A., M. E. Solak, and D. P. Yorty, 2005: Is air pollution impacting winter orograhic precipitation in Utah? Weather modification association. *J. Wea. Modif.,* **37,** 14–20.

Gunn, R., and B. B. Phillips, 1957: An experimental investigation of the effect of air pollution on the initiation of rain. *J. Meteor.,* **14,** 272–280.

Jirak, I. L., and W. R. Cotton, 2006: Effect of air pollution on precipitation along the Front Range of the Rocky Mountains. *J. Appl. Meteor.,* **45,** 236–245.

Khain, A., D. Rosenfeld, and A. Pokrovsky, 2005: Aerosol impact on the dynamics and microphysics of convective clouds. *Quart. J. Roy. Meteor. Soc.,* **131,** 2639–2663.

Levin, Z., E. Ganor, and V. Gladstein, 1996: The effects of desert particles coated with sulfate on rain formation in the eastern Mediterranean. *J. Appl. Meteor.,* **35,** 1511–1523.

Mantua, N. J., S. R. Hare, Y. Zhang, J. M. Wallace, and R. C. Francis, 1997: A Pacific interdecadal climate oscillation with impacts on salmon production. *Bull. Amer. Meteor. Soc.,* **78,** 1069–1079.

Ropelewski, C. F., and P. D. Jones, 1987: An extension of the Tahiti–Darwin Southern Oscillation index. *Mon. Wea. Rev.,* **115,** 2161–2165.

Rosenfeld, D., 1999: TRMM observed first direct evidence of smoke from forest fires inhibiting rainfall. *Geophys. Res. Lett.,* **26,** 3105–3108.

——, 2000: Suppression of rain and snow by urban air pollution. *Science,* **287,** 1793–1796.

——, and W. L. Woodley, 2003: Closing the 50-year circle: From cloud seeding to space and back to climate change through precipitation physics. *Cloud Systems, Hurricanes, and the Tropical Rainfall Measuring Mission (TRMM): A Tribute to Dr. Joanne Simpson*, *Meteor. Monogr.,* No. 51, Amer. Meteor. Soc., 59–80.

——, R. Lahav, A. P. Khain, and M. Pinsky, 2002: The role of sea-spray in cleansing air pollution over ocean via cloud processes. *Science,* **297,** 1667–1670.

Rudich, Y., O. Khersonsky, and D. Rosenfeld, 2002: Treating clouds with a grain of salt. *Geophys. Res. Lett.,* **29,** 2060, doi:10.1029/2002GL016055.

Silverman, B. A., 2003: A critical assessment of hygroscopic seeding of convective clouds for rainfall enhancement. *Bull. Amer. Meteor. Soc.,* **84,** 1219–1230.

Squires, P., 1958: The microstructure and colloidal stability of warm clouds. *Tellus,* **10,** 256–271.

U.S. Census Bureau, cited 2004a: Selected historical decennial census population and housing counts. [Available online at http://www.census.gov/population/www/censusdata/hiscendata.html.]

——, cited 2004b: Population estimates, national and state population estimates. [Available online at http://www.census.gov/popest/estimates.php.]

Zhang, Y., J. M. Wallace, and D. S. Battisti, 1997: ENSO-like interdecadal variability: 1900–93. *J. Climate,* **10,** 1004–1020.